

Article

Chemical Weathering Rates of Soils Developed on Eocene Marls and Sandstones in a Mediterranean Catchment (Istria, Croatia)

Ozren Hasan , Slobodan Miko *, Saša Mesić and Zoran Peh

Croatian Geological Survey, Sachsova 2, 10000 Zagreb, Croatia; ohasan@hgi-cgs.hr (O.H.); zpeh@hgi-cgs.hr (Z.P.)
* Correspondence: smiko@hgi-cgs.hr; Tel.: + 385-1616-0888

Abstract: Physical and chemical weathering, together with biological and biochemical processes, form soil from bedrock and strongly influence the chemical composition of natural waters. Erosive processes, primarily through the agents of running water and wind, remove the products of weathering from catchments. The aim was to determine the chemical weathering of minerals because of changes in land-use and natural forestation in two small neighboring catchments of the rivers Argilla and Bazuja. Agricultural land-use practice is very intense in the Argilla catchment, while the Bazuja catchment's arable land is mostly abandoned, with progressive forestation. Chemical weathering in soils and sediments was evaluated with the aid of bulk chemistry analysis focused on major elements, trace elements, and zirconium. Weathering indices, mass balance, and strain were calculated. The abandonment of arable land and intense forestation in the Bazuja catchment caused increased chemical weathering with the loss of base cations (Ca and Mg) and enrichment of conservative elements (Zr and Ti) in surface horizons. EIC and MTF values are positive (enrichment) in areas with agricultural activities, while forested areas show negative values (loss). A comparison of the oldest and youngest parts of the overbank sediment profiles in the swallow hole zone and stream sediments shows that chemical and mechanical weathering in the Bazuja catchment was similar to present weathering in the Argilla catchment, while agriculture was active in the Bazuja catchment. The integrated knowledge gained in small catchment studies can be broadly applicable to larger systems.



Citation: Hasan, O.; Miko, S.; Mesić, S.; Peh, Z. Chemical Weathering Rates of Soils Developed on Eocene Marls and Sandstones in a Mediterranean Catchment (Istria, Croatia). *Land* **2023**, *12*, 913. <https://doi.org/10.3390/land12040913>

Academic Editor: Augusto Pérez-Alberti

Received: 24 March 2023

Revised: 13 April 2023

Accepted: 17 April 2023

Published: 19 April 2023



Copyright: © 2023 by the authors. Licensee MDPI, Basel, Switzerland. This article is an open access article distributed under the terms and conditions of the Creative Commons Attribution (CC BY) license (<https://creativecommons.org/licenses/by/4.0/>).

Keywords: chemical weathering; small catchment; land-use change; weathering index; mass balance; strain; forestation

1. Introduction

Abandoning arable land and natural forestation has a significant effect on weathering. Two catchments in the Dragonja watershed were selected as representative sites to study the effects of natural reforestation and agriculture on chemical weathering and physical erosion. This watershed was selected because, in the short period of approximately ten years after World War II, significant changes in reforestation occurred [1,2]. Due to political but also economic conditions, there was an exodus of the local population, which caused abandonment or a change in the use of the land. The reforestation has led to a decrease in suspended sediment supply to the lower reaches of the Dragonja catchment [2–4]. Deforestation is an ongoing land cover change process in Europe [5] with the effects of soil erosion, degradation of soil properties, and nutrient losses [6–9]. The impacts of soil erosion go beyond the denudation of topsoil and reduction of soil fertility [6,10]. It results in major land and environmental degradation, and can lead to increased pollution and sedimentation in streams and rivers, causing declines in the ecosystem [10,11]. Erosion can create an increased sediment load, which directly impacts the flood-carrying capacity of streams and rivers and can eventually lead to flooding [11,12]. Since 1990, an opposite process, similar to the one in the Dragonja catchment, has been taking place in the EU, where forests increased by 10% between 1990 and 2020 [13]. Industrialized countries increased the

amount of arable land and successively cut down forests and other natural habitats [14,15]. Extensive European deforestation is considered to have started in 1000 BC [16,17]. The spread of vegetation cover is a crucial factor governing physical erosion [18,19] and chemical weathering [20,21].

The weathering processes of marls and sandstones (flysch deposits of Istria) have been intensively studied in terms of physical erosion since the intense denudation processes lead to the formation of badlands [3,22–25]. Studies in the Slovenian part of the Dragonja flysch basin [2,26] found that most of the suspended sediments were sourced from the flysch badland hillslopes. Chemical weathering and soil formation on the flysch deposits have not been studied as extensively. The available data is related to regional soil geochemical surveys [27–30] and provenance analysis related to the formation of terra rossa soils on neighboring karst [31–33]. Due to the strong dynamism involved in the process of rapid erosion and the mixing of fresh parent material with the already formed regolith, soils that evolved on flysch (mostly rendzinas) are typically “immature”, that is, incipient and undeveloped [30]. This process is well recognized on the Istrian Peninsula [34,35]. When compared with “mature” soils that have evolved over carbonate bedrock, undeveloped (flysch-derived) soils typically have stable or even depleted concentrations of trace elements and higher levels of carbonate minerals as a result of poor drainage and leaching [30].

Chemical weathering and physical erosion are related processes that control soil development, deliver sediments and solutes to the riparian zone and streamwater, and form the landscape [36–41]. Various approaches to chemical weathering estimations are commonly used through the analysis of the bulk chemistry of weathered catena. Weathering indices can be based on the approach used by monitoring the decomposition of an unstable mineral or tracing the mass transfer of a labile element. The most common weathering indexes used are CIA = $(Al_2O_3 \times 100 / (Al_2O_3 + CaO + Na_2O + K_2O))$ [42], PIA = $(Al_2O_3 - K_2O) \times 100 / (Al_2O_3 + CaO + Na_2O - K_2O)$ [43], CIW = $Al_2O_3 \times 100 / (Al_2O_3 + CaO + Na_2O)$ [44], and WIP = $100 [(2 Na_2O / 0.35) + (MgO / 0.9) + (2 K_2O / 0.25) + (CaO / 0.7)]$ [45]. Labile element mobility during weathering can be characterized by the mass transfer coefficient (eluvial-illuvial coefficient, EIC [36,46,47]) and mass-transport function (τ) [47–49], assuming Zr as the conservative component and the saprolite-rock boundary samples as the least weathered [36,47,50–52]. The importance of parent materials in the early stages of soil formation is stressed by [53] while other processes influenced by vegetation and hydrology become the main factors of chemical weathering.

This article represents an attempt to quantify the weathering of two catchments with the same heterogeneous lithology, comprising an alternation of marl and calcareous sandstones (flysch) and different land cover and land-use practices. Changes in long-term weathering rates were evaluated through a comparison of the molar ratios of major elements [49,54,55] in recent stream sediments, overbank sediment profiles in swallow hole zones, and soil profiles.

The elemental ratios show that stream sediments derived after storm events are mainly derived from less weathered material and plot close to calcarenite/marl composition. Molar ratios of the youngest and oldest parts of the ≈ 5 m high overbank sediment profile in the swallow hole zone of the river Bazuja showed that the oldest deposited sediments are similar to present-day Argilla catchment soils. The younger overbank sediments geochemically correspond with the soils of the eastern part of the Bazuja catchment. Natural forestation and the abandonment of arable lands have a critical effect on chemical weathering rates in these catchments, causing a loss of base cations Ca and Mg from the top 50 cm of soil profiles and increasing the overall acidification. Rock and mineral weathering, as well as soil formation, are strongly affected by biomass elemental uptake, significantly increasing weathering [21]. Results show higher losses in the river Bazuja catchment, and even enrichment in some parts of the river Argilla catchment compared with c-horizon.

2. Investigation Area

The studied area is located in the northern part of the Istrian peninsula (Republic of Croatia), as seen in Figure 1a. The area of interest is the Dragonja River catchment, or more accurately, the small catchments of the river Argilla and sinking river Bazuja, with a total area of approximately 35 km² (Figure 1b). River Argilla is the tributary of the river Dragonja and river Bazuja is an influent river with allogenic recharge and a wide floodplain in the swallow hole (ponor) zone. Dragonja is a borderline river, with a catchment area of approximately 100 km². One-quarter of that area is in Croatia and the rest is in Slovenia.

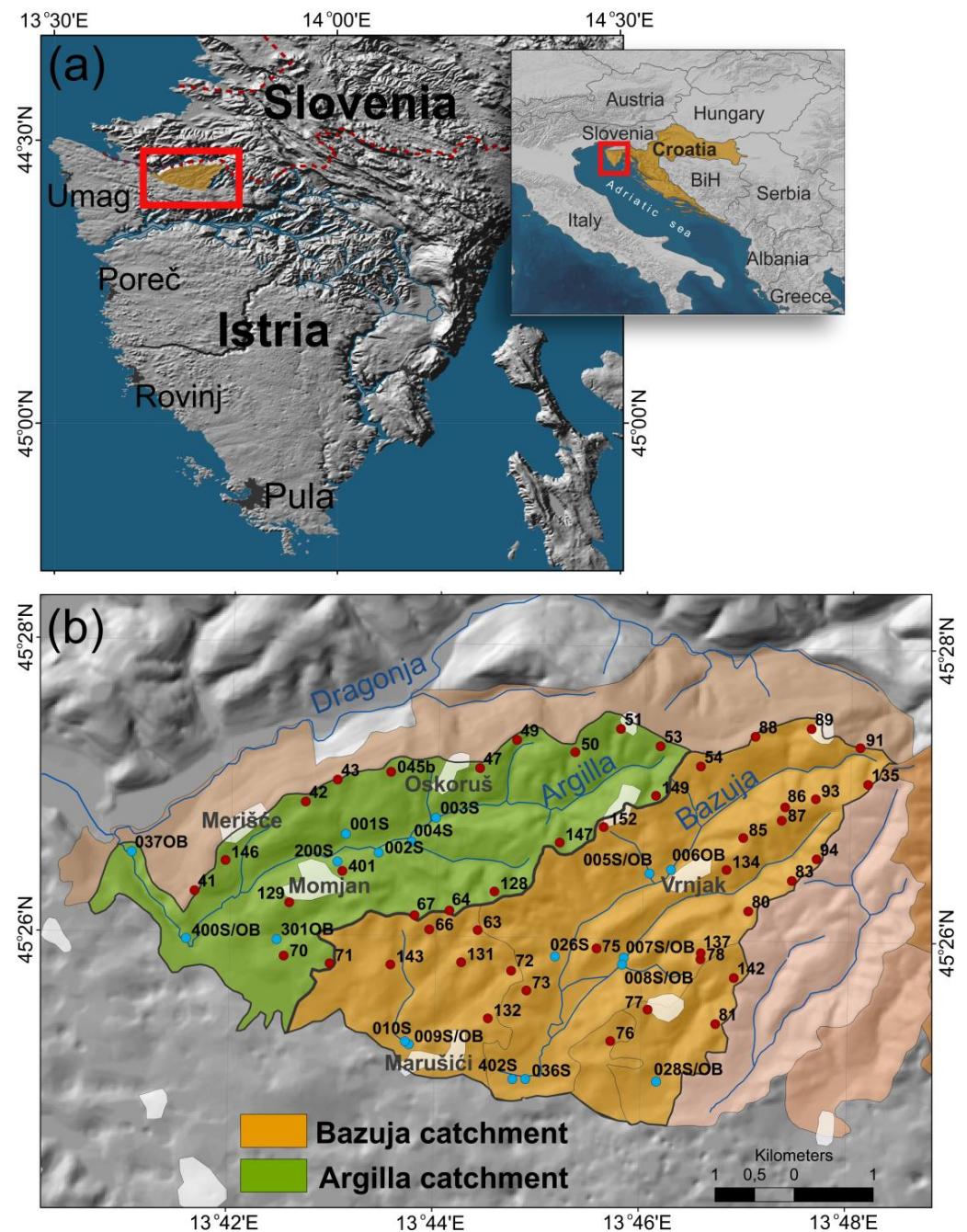


Figure 1. (a) General location of the study area; (b) rivers Argilla and Bazuja, with their catchments and marked sampling sites of soil profiles (red circles) and stream sediments, overbank sediments, and water (blue circles).

Catchments differ by the intensity of agricultural activity: the Argilla catchment is characterized by intensive cultivation, while the Bazuja River catchment is predominantly abandoned. The catchments are a part of the accumulation-denudation type of morpho-structure characterized by rapid denudation processes developed on Eocene flysch deposits [22,23,56]. The flysch bedrock comprises turbidite deposits with alternating layers of marls and arenites that are individually and frequently thinner than 30 cm. The calcarenites contain quartz, feldspar, mica grains, and lithoclasts of both carbonate and silicate rocks (chert, quartzite, and schist). Carbonate nummulite breccia beds within the marls and sandstone are also found. The arenite to marl thickness ratio (A/M) in the flysch deposits ranges from 1: 2 to 1: 50 [57,58]. Soils in the Argilla catchment are developed predominantly on Upper Eocene bedrock, while soils in the Bazuja catchment overlay Middle Eocene sedimentary rocks.

The investigated catchments are covered with three dominant soil types: regosol (sirozem), rendzina on flysch, or rigosol (anthropogenic soil).

The climate of the Istrian peninsula is affected by the north Adriatic Sea and the Mediterranean in general, but also by the European interior, especially the Alps, the Dinarides, and the River Po valley. According to Köppen classification, the peninsula has a Cfa climate type. In Thornthwaite's classification, the climate is perihumid to locally humid. During the summer, the Istrian peninsula is under the influence of the Azores cyclone, and during the winter, the effect of the Siberian anticyclone prevails. The Island anticyclone and frontal disturbances connected with it affect weather conditions throughout the whole year, especially during the winter [59]. Istria is characterized by a warm and dry summer and a cold and moist winter, typical of a sub-Mediterranean climate.

3. Materials and Methods

3.1. Sampling Strategy

In this study, soils, stream sediments, overbank sediments, and river water were sampled. Soil material was collected from 32 excavated profile pits. Samples were taken at depths of 0–5 cm (O and A horizons), 5–20 cm (B-horizons), and 40–50 cm (B/C horizons). Sampling depth intervals were based on standard methods of soil sampling for the changes of organic carbon stock in mineral soils [60] and the Geochemical Atlas of Croatia [27]. Approximately 3 kg of soil materials/samples were collected per soil horizon. If the bedrock was not reached, samples from horizons deeper than 50 cm were taken. Samples from deeper horizons were then collected at 20-cm intervals (e.g., 50–70 cm, 70–90 cm, etc.). At specific locations, parent rocks (marls and sandstones) were sampled, fresh and weathered. Soils were sampled, taking the land-use into account. Due to this, profiles were made in meadows, vineyards, and forests (deciduous and conifers). Soil color was determined using the Munsell color chart (1984). Colors vary (Supplement Table S1) from 10 YR to 5 Y, with dominant 2.5 Y colors (brown, grayish brown, and olive brown).

Stream sediments were sampled in all active streams in 15 locations. Overbank sediments were sampled in four locations: on the inlet of Argilla with Dragonja (site 37, Figure 1), on the location of the periodically flooded area of the Argilla River (site 400, Figure 1), and the swallow hole near the village of Marušići and Bazuja River (sites 009 and 402, Figure 1) [61]. Sediments were sampled in profile pits at 10 cm intervals. Samples in the Bazuja River swallow hole were taken from the ~15 m high overbank sediment profile.

3.2. Soil Geochemistry

Chemical analyses of the soil samples were determined by ICP-AES (major elements, Ba, Ni, S) and ICP-MS (Co, Hf, Rb, Sr, Ta, Th, U, V, W, Zr, REE, Mo, Cu, Pb, Zn, Ni, As, Cd, Ag, Au, Hg). Air-dried samples were dissolved using LiBO₂ at 400 °C or a mixture of HCl-HNO₃-H₂O at 95 °C. Total C and S were determined using the Elemental analyzer LECO CNS-2000 (LECO Corporation, St. Joseph, MI, USA). Soil pH was determined from air-dried samples using a soil/solution ratio of 1:2.5. Major element composition, pH, and

color of samples are presented in Supplement Table S1. Bulk density was determined from selected soil samples using the clod method [62].

3.3. Theoretical Background

Analysis of bulk soil chemistry (major elements and trace elements) is the most common method of determining rates of chemical weathering [47,63]. The mobility of elements during weathering is influenced by three main factors: pH, ion potential, and redox soil conditions. Evaluation of the degree of weathering in the soil profile is possible in several ways. To calculate the mass change of an element, it is necessary to compare its change in concentration with the concentration of an immobile element. Usually, Zr and Ti are considered elements that are not mobile during weathering [37,64,65]. In this study, Zr is used as an immobile element. Almost all Zr in flysch occurs in the mineral zircon (ZrSiO_4), which is resistant to low-temperature near-to-surface weathering.

The basic approach in calculating mass changes includes the comparison of ratios of weatherable (mobile) and conservative (immobile) constituents in the soil horizons with the ratio of the same elements in the parent sedimentary deposit or least weathered horizon. In this study, the calculations were made based on the assumption that the initial material was the least weathered, containing unweathered rock fragments (usually a mixture of fine-grained marl and coarse fragments of calcareous sandstone). The advantage of using the individual C-horizon as a satisfactory parent composition source is that the variation of the marls and calcarenites is incorporated directly into the calculation, although a bias is also introduced if the C-horizons are weathered to varying degrees, which must not be neglected.

Two methods were used in calculating weathering rates: the eluvial-illuvial index [36,46,47] and the mass-transport function [47,48]. The equation for calculating EIC is:

$$\text{EIC (\%)} = \frac{(X_A/S_A)}{(X_m/S_m)} - 1 \times 100$$

where X = observed element oxide, S = stable element oxide, A = observed horizon, m = parent rock or C-horizon.

Negative values represent a loss of the element observed and positive values represent a gain compared with the parent rock or C-horizon. The amount of the element that remains in the soil was calculated for each profile at two depths. The fractional mass of non-conservative elements was calculated based on Zr as the conservative element.

The second method used for calculating weathering rates was the mass-transport function, which is calculated as [66,67]:

$$\tau_A = \left(\frac{\delta_A X_A}{\delta_m X_m} (\varepsilon_A + 1) \right) - 1$$

where δ = bulk density, X = concentration of the observed element, A = observed horizon, m = parent rock or C-horizon, ε = strain.

Calculated values show if the element is immobile ($\tau_A = 0$), if there is enrichment in the observed element ($\tau_A > 0$), or if there is a loss of it ($\tau_A < 0$). The value $\tau_A = -1$ represents a complete removal of the element in the observed horizon.

To calculate the volumetric strain of an immobile element, it can be assumed that, since it is immobile, $\tau = 0$. In that case, volumetric strain can be calculated as [67]:

$$\varepsilon_A = \frac{\delta_m I_m}{\delta_A I_A} - 1$$

where δ = bulk density, I = concentration of an immobile element, A = observed horizon, m = parent rock or C-horizon, ε = volumetric strain.

Positive strain values denote dilations and negative strain values denote collapse. Bulk density was measured on 55 samples. Each value was calculated as the average of three measured samples.

After calculating weathering rates by these two methods, the obtained results were identical for all the samples that bulk density was measured on. Therefore, to make data presentation simpler, only EIC values will be mentioned in this paper, and the EIC and MTF values are shown in Supplementary Table S1.

Weathering rates may also be calculated as a comparison of the molar ratios of the oxides of major elements [49,68], comparing recent stream sediments, overbank sediment profiles, and soil profiles. Usually, ratios (i) $\text{SiO}_2/\text{Al}_2\text{O}_3$, (ii) $\text{SiO}_2/\text{Fe}_2\text{O}_3$, (iii) $\text{SiO}_2/(\text{Fe}_2\text{O}_3 + \text{Al}_2\text{O}_3)$, (iv) $\text{SiO}_2/(\text{Fe}_2\text{O}_3 + \text{Al}_2\text{O}_3 + \text{TiO}_2)$, (v) $(\text{K}_2\text{O} + \text{Na}_2\text{O} + \text{CaO} + \text{MgO})/\text{Al}_2\text{O}_3$, (vi) $(\text{K}_2\text{O} + \text{Na}_2\text{O} + \text{CaO} + \text{MgO})/(\text{Fe}_2\text{O}_3 + \text{Al}_2\text{O}_3 + \text{TiO}_2)$, (vii) $\text{Na}_2\text{O}/\text{K}_2\text{O}$, (viii) Ba/Sr are used [68]. The values of indices (i) through (iv) should generally be lower with the increase in weathering. Ratios (v) and (vi) present an estimate of cation loss, while the index (i) estimates the formation of clay minerals [47]. Ratio (ii) represents the degree of formation of pedogenetic Fe-oxides and hydroxides. Changes in the ratio (vii) can point to cation substitution and their fixation on clay minerals [69]. The molar ratio (viii) is an estimate of leaching and can point out the time of soil formation [68]. All ratios can be used for parent rocks, weathered rocks, and soils.

3.4. Construction of Graphs and Maps

Mathematical and statistical computations were performed using the Agisoft STATISTICA version 7. Graphs were created in STATISTICA version 7 and MS Excel version 2016. Spatial analyses and maps were generated using ESRI ArcGIS 10.2.1. Interpolation of data was carried out in the ArcGIS extension Geostatistical Analyst using the Empirical Bayesian Kriging method with a grid of $15\text{ m} \times 15\text{ m}$.

4. Results

4.1. Chemical Soil Composition of the Catchments and Their Comparison

Weathering indices in the Argilla catchment show a visible increase in proportions of $\text{SiO}_2/\text{Al}_2\text{O}_3$, $\text{SiO}_2/\text{Fe}_2\text{O}_3$, and $\text{SiO}_2/(\text{Fe}_2\text{O}_3 + \text{Al}_2\text{O}_3 + \text{TiO}_2)$ (Figure 2, Table 1) towards the surface. Ratio Ba/Sr decreases with depth, while ratios $(\text{K}_2\text{O} + \text{Na}_2\text{O} + \text{CaO} + \text{MgO})/\text{Al}_2\text{O}_3$ and $(\text{K}_2\text{O} + \text{Na}_2\text{O} + \text{CaO} + \text{MgO})/(\text{Fe}_2\text{O}_3 + \text{Al}_2\text{O}_3 + \text{TiO}_2)$ (Figure 2, Table 1) increase. Differences in the $\text{Na}_2\text{O}/\text{K}_2\text{O}$ ratio are minor (Table 1). EIC in the Argilla catchment shows enrichment of SiO_2 (Figure 3, Table 2) and Na_2O (Figure 4, Table 2) in samples closer to the surface. EIC of Al_2O_3 and MgO (Figure 5, Table 2) shows depletion compared with the c-horizon, which is larger in the b-horizon. CaO shows minor enrichment in the b-horizon and is slightly depleted in the a-horizon. (Figure 6, Table 2). EIC Fe_2O_3 (Figure 7, Table 2) shows enrichment compared with the c-horizon.

Table 1. Mean weathering index values in soil profiles (a, b, c, and d horizons), stream sediments (sa), and not weathered marls (ar-lp) and sandstones (ar-ps) in the river Argilla catchment.

Argilla Catchment/Horizon	a	b	c	d	sa	ar-ps	ar-lp
$\text{SiO}_2/\text{Al}_2\text{O}_3$	8.90	8.90	8.78	7.58	10.87	10.89	6.91
$\text{SiO}_2/\text{Fe}_2\text{O}_3$	6.93	6.91	6.80	5.96	8.44	8.46	5.59
$\text{SiO}_2/(\text{Fe}_2\text{O}_3 + \text{Al}_2\text{O}_3 + \text{TiO}_2)$	6.53	6.52	6.41	5.64	7.90	8.00	5.31
$(\text{K}_2\text{O} + \text{Na}_2\text{O} + \text{CaO} + \text{MgO})/\text{Al}_2\text{O}_3$	2.80	3.03	2.94	4.88	3.69	8.80	5.75
$(\text{K}_2\text{O} + \text{Na}_2\text{O} + \text{CaO} + \text{MgO})/(\text{Fe}_2\text{O}_3 + \text{Al}_2\text{O}_3 + \text{TiO}_2)$	2.07	2.23	2.15	3.71	2.69	6.45	4.42
$\text{Na}_2\text{O}/\text{K}_2\text{O}$	0.52	0.54	0.53	0.43	0.66	0.81	0.37
Ba/Sr	2.20	2.26	2.07	1.50	1.45	0.66	0.66

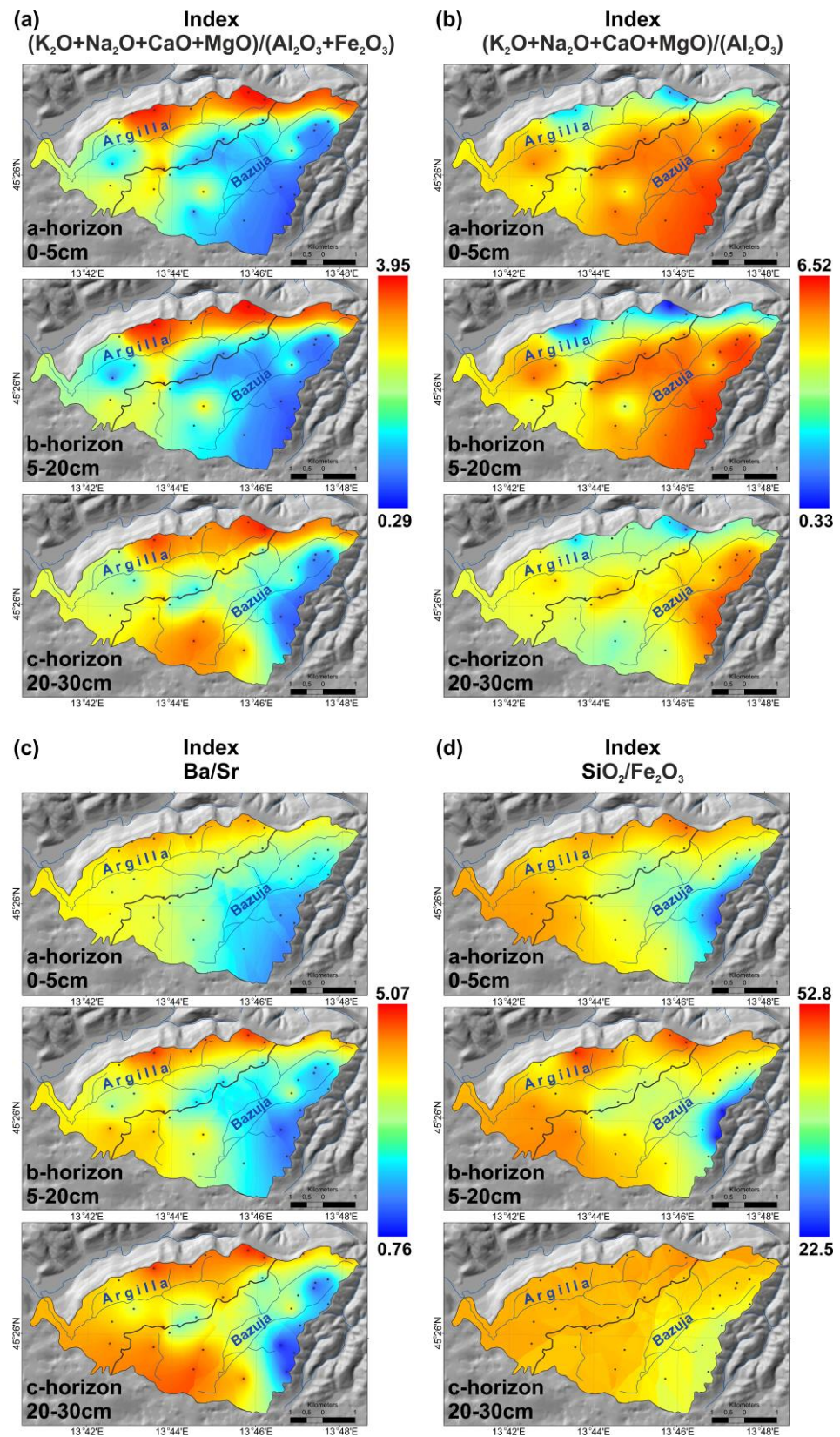


Figure 2. Distribution of weathering indices (a) $(K_2O + Na_2O + CaO + MgO)/(Al_2O_3 + Fe_2O_3)$; (b) $(K_2O + Na_2O + CaO + MgO)/Al_2O_3$; (c) Ba/Sr ; (d) SiO_2/Fe_2O_3 in different soil horizons in the rivers' Argilla and Bazuja's catchments.

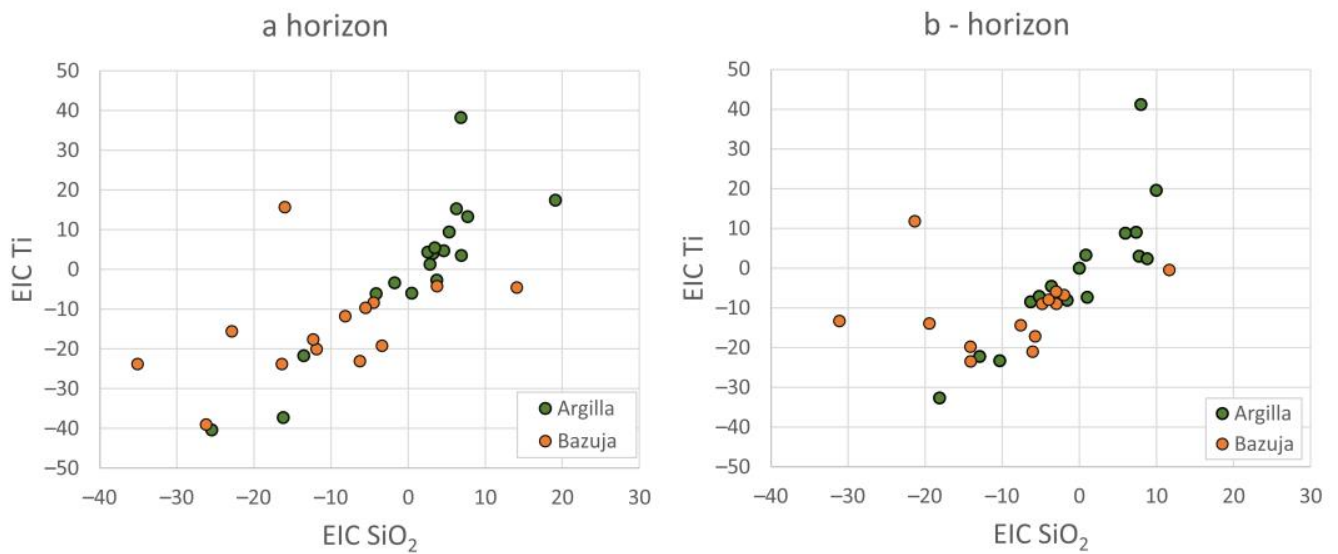


Figure 3. Distribution of calculated EIC SiO₂ compared with EIC Ti in (a) and (b) soil horizons in the rivers' Argilla and Bazuja's catchments.

Table 2. Mean EIC values of major elements in soil profiles in river Argilla and river Bazuja.

EIC Index	Argilla		Bazuja	
	a-Horizon	b-Horizon	a-Horizon	b-Horizon
SiO ₂	0.66	0.16	−10.76	−8.90
Al ₂ O ₃	−0.19	−0.48	−28.31	−22.99
CaO	−3.73	4.71	−27.05	−33.40
MgO	−0.46	−2.84	−35.79	−31.91
K ₂ O	4.72	−1.06	−28.25	−26.67
Na ₂ O	2.59	1.01	−15.74	−14.42
Fe ₂ O ₃	1.12	2.18	−24.68	−20.11

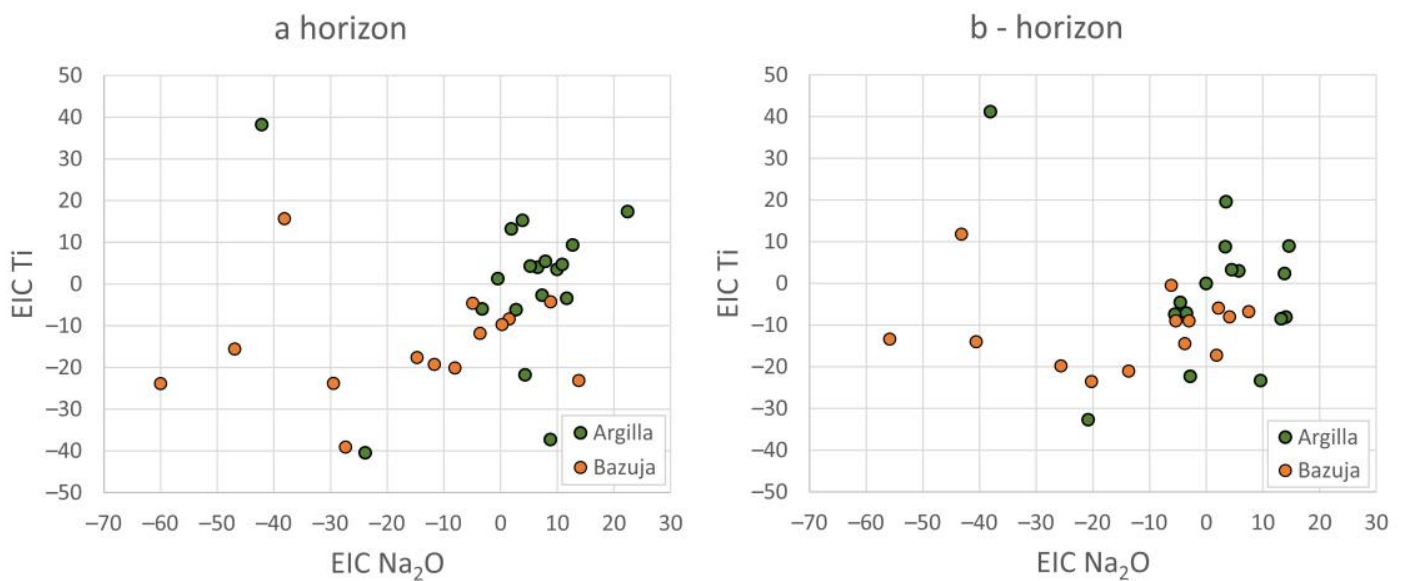


Figure 4. Distribution of calculated EIC Na₂O compared with EIC Ti in (a) and (b) soil horizons in the rivers' Argilla and Bazuja's catchments.

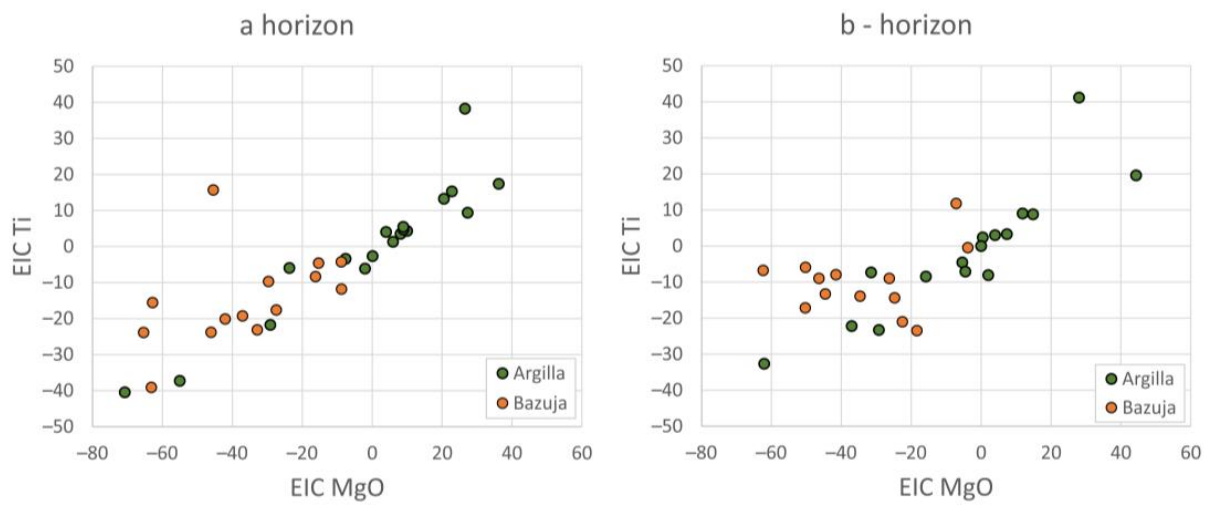


Figure 5. Distribution of calculated EIC MgO compared to EIC Ti in (a) and (b) soil horizons in the rivers Argilla and Bazuja's catchments.

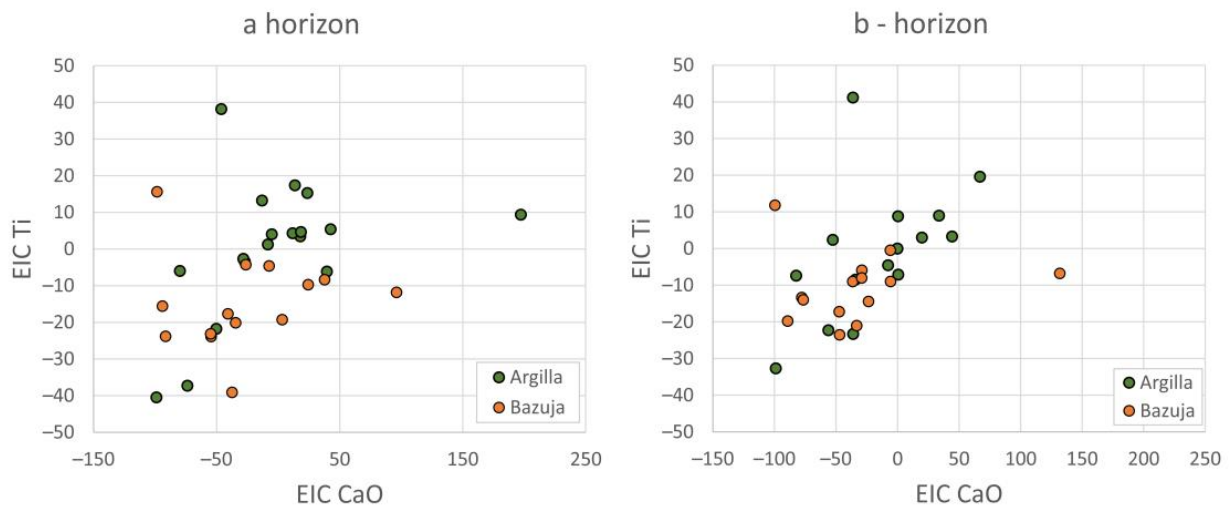


Figure 6. Distribution of calculated EIC CaO compared to EIC Ti in (a) and (b) soil horizons in the rivers Argilla and Bazuja's catchments.

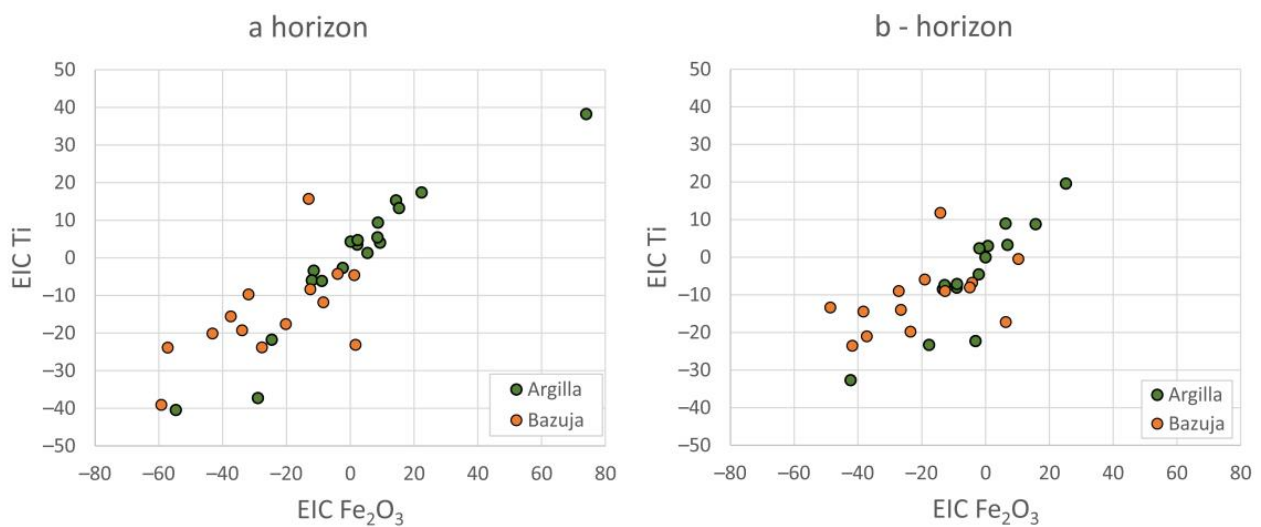


Figure 7. Distribution of calculated EIC Fe₂O₃ compared to EIC Ti in (a) and (b) soil horizons in the rivers Argilla and Bazuja's catchments.

In the Bazuja River catchment, values of weathering indices in the a, b, and c horizons are higher towards the surface in ratios $\text{SiO}_2/\text{Al}_2\text{O}_3$, $\text{SiO}_2/\text{Fe}_2\text{O}_3$, and $\text{SiO}_2/(\text{Fe}_2\text{O}_3 + \text{Al}_2\text{O}_3 + \text{TiO}_2)$, while the values of ratios $(\text{K}_2\text{O} + \text{Na}_2\text{O} + \text{CaO} + \text{MgO})/(\text{Fe}_2\text{O}_3 + \text{Al}_2\text{O}_3 + \text{TiO}_2)$ increase in the lower horizons (Figure 2, Table 3). The Ba/Sr (Figure 2c, Table 3) ratio is somewhat diminished in sample d and is similar in the rest of the profile. R. Bazuja profiles show a loss of all calculated EIC values compared with c-horizons (Figures 3–7, Table 2). Depletion of CaO (Figure 6, Table 2) is greater in the b-horizon, while other base cations are more depleted closer to the surface.

Table 3. Mean weathering index values in soil profiles (a, b, c, and d horizons), stream sediments (sb), older (bs) and younger (bm) ponor (swallow hole) overbank sediments, and not weathered marls (ar-lp) and sandstones (ar-ps) in the river Bazuja catchment.

Bazuja/Horizon	a	b	c	d	sb	bs	bm	br-ps	br-lp
$\text{SiO}_2/\text{Al}_2\text{O}_3$	11.70	10.96	9.33	10.57	10.56	11.61	10.31	12.56	6.62
$\text{SiO}_2/\text{Fe}_2\text{O}_3$	9.10	8.54	7.26	8.29	7.99	9.05	8.13	9.37	5.47
$\text{SiO}_2/(\text{Fe}_2\text{O}_3 + \text{Al}_2\text{O}_3 + \text{TiO}_2)$	8.41	7.92	6.78	7.68	7.46	8.45	7.54	8.87	5.18
$(\text{K}_2\text{O} + \text{Na}_2\text{O} + \text{CaO} + \text{MgO})/\text{Al}_2\text{O}_3$	1.18	1.10	1.45	0.52	2.65	2.52	0.90	12.99	7.06
$(\text{K}_2\text{O} + \text{Na}_2\text{O} + \text{CaO} + \text{MgO})/(\text{Fe}_2\text{O}_3 + \text{Al}_2\text{O}_3 + \text{TiO}_2)$	0.85	0.80	1.07	0.38	1.87	1.83	0.66	9.17	5.52
$\text{Na}_2\text{O}/\text{K}_2\text{O}$	0.68	0.67	0.57	0.64	0.69	0.71	0.76	0.90	0.35
Ba/Sr	3.76	3.85	3.74	4.94	1.59	1.40	3.22	0.34	0.49

As is visible in Figure 8, the ratios $\text{SiO}_2/\text{Al}_2\text{O}_3$, $\text{SiO}_2/\text{Fe}_2\text{O}_3$, $\text{SiO}_2/(\text{Fe}_2\text{O}_3 + \text{Al}_2\text{O}_3 + \text{TiO}_2)$, Ba/Sr, and $\text{K}_2\text{O}/\text{Na}_2\text{O}$ show higher values in the Bazuja River catchment. Ratios $(\text{K}_2\text{O} + \text{Na}_2\text{O} + \text{CaO} + \text{MgO})/(\text{Fe}_2\text{O}_3 + \text{Al}_2\text{O}_3 + \text{TiO}_2)$ and $(\text{K}_2\text{O} + \text{Na}_2\text{O} + \text{CaO} + \text{MgO})/\text{Al}_2\text{O}_3$ have higher values in the agriculturally active river Argilla catchment. EIC calculations show enrichment in the a-horizon in both catchments in areas with active agriculture, while areas covered with forest show losses in shallower horizons. Since the river Bazuja catchment is generally covered with forest and is abandoned, soils sampled in that catchment generally show a loss in EIC values in the a and b-horizons.

4.2. Chemical Composition of Stream Sediments in the Catchment and Their Comparison

By comparing the weathering indices in both catchments, it is clear that the values of the ratios $(\text{K}_2\text{O} + \text{Na}_2\text{O} + \text{CaO} + \text{MgO})/\text{Al}_2\text{O}_3$ and $(\text{K}_2\text{O} + \text{Na}_2\text{O} + \text{CaO} + \text{MgO})/(\text{Fe}_2\text{O}_3 + \text{Al}_2\text{O}_3 + \text{TiO}_2)$ (Figure 8, Tables 1 and 3) are higher in the Argilla river catchment. Ratios $\text{SiO}_2/\text{Al}_2\text{O}_3$, $\text{SiO}_2/(\text{Al}_2\text{O}_3 + \text{Fe}_2\text{O}_3)$, $\text{SiO}_2/(\text{Fe}_2\text{O}_3 + \text{Al}_2\text{O}_3 + \text{TiO}_2)$, $\text{Na}_2\text{O}/\text{K}_2\text{O}$, and Ba/Sr (Figure 8, Tables 1 and 3) are higher in the Bazuja river catchment.

All weathering indices show higher chemical weathering in the Bazuja River catchment. The range of values of weathering indices for stream sediments is visibly smaller than the range of indices for soil sediments (Figure 8).

4.3. Analysis of the Overbank Sediment Profiles in the River Bazuja Swallow Hole

If the values of the base cations of older and younger overbank sediments in location 402 in the Bazuja River swallow hole are compared (Figure 1, Tables 3 and 4), it is visible that younger sediments (marked as 402A) have lower values of SiO_2 , Al_2O_3 , Fe_2O_3 , MgO, K_2O , Na_2O , TiO_2 , Cu, Ba, Ni, and Sc, and have significantly higher values of CaO and total C. The same trend can be seen in the base cation ratios of stream sediments from the rivers Argilla and Bazuja. The composition of base cations in stream sediments of older overbank sediments is similar to the composition of base cations in Argilla River sediments (sample 009). Sediments of the river Bazuja catchment, on the other hand, have a composition very similar to more recent overbank sediments.

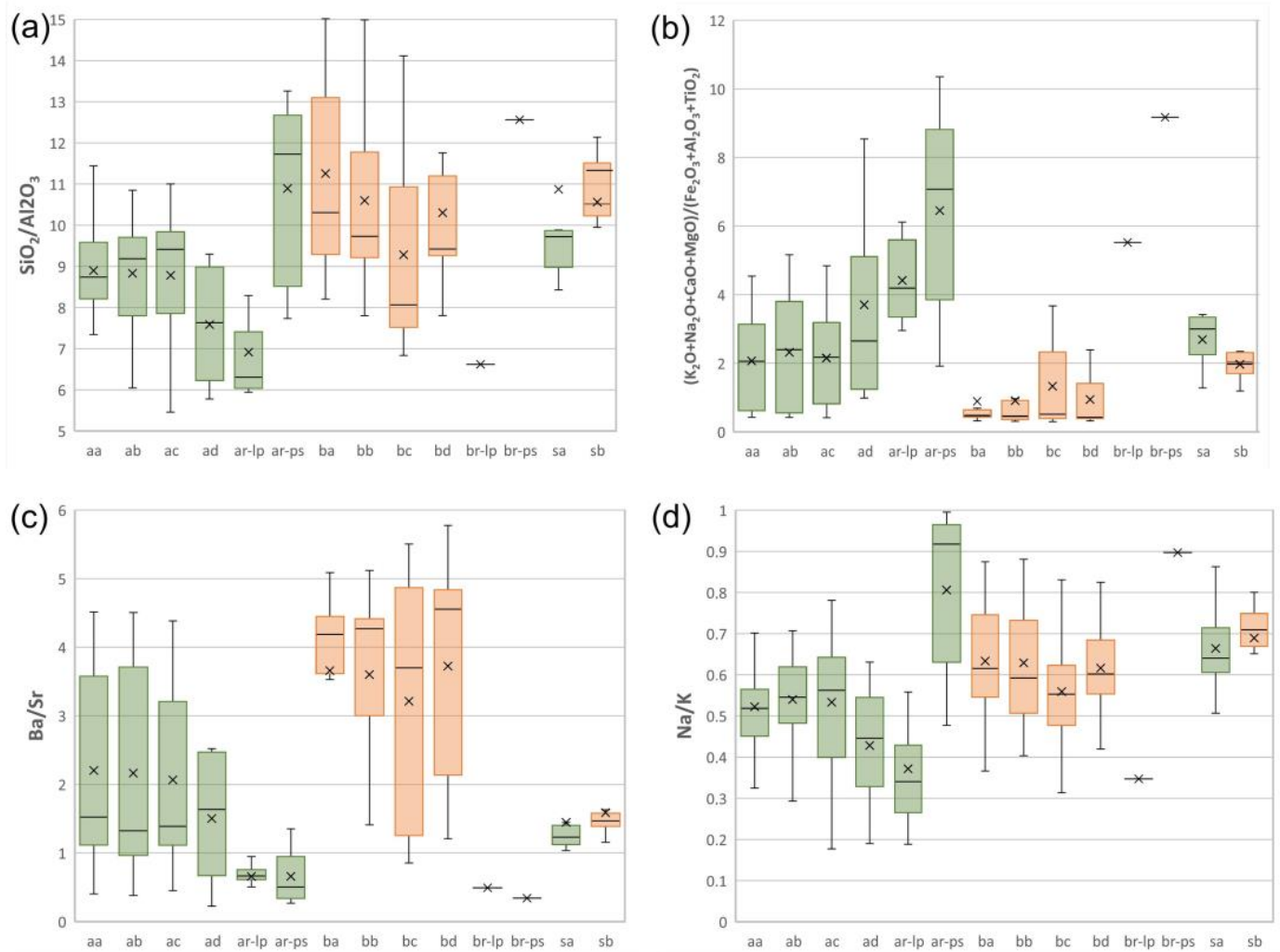


Figure 8. Distribution of weathering indices (a) $\text{SiO}_2/\text{Al}_2\text{O}_3$; (b) $(\text{K}_2\text{O} + \text{Na}_2\text{O} + \text{CaO} + \text{MgO})/(\text{Fe}_2\text{O}_3 + \text{Al}_2\text{O}_3 + \text{TiO}_2)$; (c) Ba/Sr ; (d) Na/K in Argilla and Bazuja catchment sediments (aa—a-horizon Argilla; ab—b-horizon, Argilla; ac—c-horizon, Argilla; ad—d-horizon, Argilla; ar-lp—marls, Argilla; ar-ps—sandstones, Argilla; ba—b-horizon, Bazuja; bb—b-horizon, Bazuja; bc—c-horizon, Bazuja; bd—d-horizon, Bazuja; ba-lp—marls, Bazuja; ba-ps—sandstones, Bazuja) and stream sediments of rivers Argilla (sa) and Bazuja (sb). Green-colored diagrams represent ranges of weathering indices for the Argilla River catchment. Orange-colored diagrams represent ranges of weathering indices for the Bazuja River catchment.

Table 4. The average content of major elements in older (402A) and younger (402B) overbank sediments in the river Bazuja swallow hole area compared with the average overbank sediment composition at point 009 in the river Argilla catchment.

Location	SiO_2 %	Al_2O_3 %	Fe_2O_3 %	MgO %	CaO %	Na_2O %	K_2O %	TiO_2 %	P_2O_5 %	MnO %	Ba mg/kg	Ni mg/kg	Sc mg/kg	Tot. C %	Tot. S %
402A	61.1	8.93	3.95	0.97	9.58	0.66	1.41	0.63	0.06	0.13	232.6	78.0	8.60	2.53	0.01
402B	67.2	11.06	4.66	1.05	2.33	0.79	1.57	0.85	0.08	0.13	271.2	93.8	11.00	1.84	0.03
009	47.8	8.40	4.30	1.04	17.09	0.55	1.39	0.52	0.08	0.15	208.9	86.5	8.42	4.24	0.02

Values of the weathering indices $\text{SiO}_2/\text{Al}_2\text{O}_3$, $\text{SiO}_2/(\text{Al}_2\text{O}_3 + \text{Fe}_2\text{O}_3)$, $\text{SiO}_2/(\text{Fe}_2\text{O}_3 + \text{Al}_2\text{O}_3 + \text{TiO}_2)$, $(\text{K}_2\text{O} + \text{Na}_2\text{O} + \text{CaO} + \text{MgO})/\text{Al}_2\text{O}_3$ and $(\text{K}_2\text{O} + \text{Na}_2\text{O} + \text{CaO} + \text{MgO})/(\text{Fe}_2\text{O}_3 + \text{Al}_2\text{O}_3 + \text{TiO}_2)$ are higher in samples of profile 402A, i.e., older overbank sediments (Table 3). Indices $\text{Na}_2\text{O}/\text{K}_2\text{O}$ and Ba/Sr have higher values in younger overbank sediments (402B) (Table 3).

5. Discussion

Comparing the weathering index values in both catchments, it can be observed that the values of $\text{SiO}_2/\text{Al}_2\text{O}_3$, $\text{SiO}_2/\text{Fe}_2\text{O}_3$, $\text{SiO}_2/(\text{Fe}_2\text{O}_3 + \text{Al}_2\text{O}_3 + \text{TiO}_2)$ (Tables 1 and 3, Figure 2) and Ba/Sr (Figure 2) are significantly higher in the Bazuja River catchment. Values of $(\text{K}_2\text{O} + \text{Na}_2\text{O} + \text{CaO} + \text{MgO})/\text{Al}_2\text{O}_3$ and $(\text{K}_2\text{O} + \text{Na}_2\text{O} + \text{CaO} + \text{MgO})/(\text{Fe}_2\text{O}_3 + \text{Al}_2\text{O}_3 + \text{TiO}_2)$ are significantly higher in the Argilla River catchment (Tables 1 and 3, Figure 2). EIC values in the Bazuja River catchment are visibly lower compared with the c-horizon, while the difference in the Argilla River is much smaller; even a- and b-horizons have higher values than the c-horizon. Enrichment of a- and b-horizons in the Argilla River catchment (Figures 4–7) is probably caused by agricultural activities. Agricultural activities cause an increase in the amount of fine parent rock particles in the soil that leads to mass balance values that are approximately equal to zero or even positive at horizons of 0–5 cm and 20–40 cm. This observation differs from the interpretation in [70], where they explain the relationships between eroding processes and chemical weathering in the sense that erosion constantly supplies fresh weatherable minerals from below the surface and that weathering reactions disintegrate bedrock to sustain physical processes of material production and erosion. In their modeling approach, [71] showed that faster erosion rates do not have to lead to faster rates of chemical denudation. Slope orientation and exposure, as demonstrated by [72], can also influence the rates of chemical weathering, but such differences were not observed in the studied catchments. At the same time, in the forested Bazuja River catchment, losses in the same horizons are high because of higher soil acidity (Figure 9), so cations are “washed out” of the catchment by water. The methods proposed by [73] i.e., solute-based watershed geochemical mass-balance methods, should be a powerful and accurate technique for quantifying mineral weathering rates in the field and will be applied in the future. Data on base cation distribution, trace elements, and weathering indices in two catchments and their comparison point out that the abandonment of arable lands and natural forest progression over abandoned olive groves, gardens, and fields in the Bazuja River catchment have a significant influence on the rate of chemical weathering [21]. This resulted in the leaching of Ca and Mg and the enrichment of conservative elements Zr and Ti in horizons in topsoils and surface horizons. Base cation loss also causes a soil pH decrease, as seen in Figure 9, where the Bazuja River catchment stands out with lower pH values. Plants also have a large effect on pH lowering in soils by producing humic acids [74,75]. The influence of vegetation cover induced a higher production of organic and chelating ligands in the soil solution, which can cause significant changes in weathering rates within short periods of approximately 100 years [76].

Copper concentrations are increased in the Argilla River catchment, which could be expected because of intensive grapevine cultivation and its treatment with copper-based solutions, which, after spraying, easily get into the ground. With depth, the copper concentration decreases. In the SE part of the Bazuja River catchment, at a depth of 40–50 cm, there is also a visible copper anomaly. Such a local anomaly could be explained by the growth of grapevines in the past before the abandonment of the area. Lead concentrations are increased in the Bazuja River catchment as a consequence of atmospheric and anthropogenic factors. Forests can act as a filter that retains a significant amount of atmospheric particles, a large portion of which are anthropogenic. During rainfall, particles are washed out and concentrated on the ground [77].

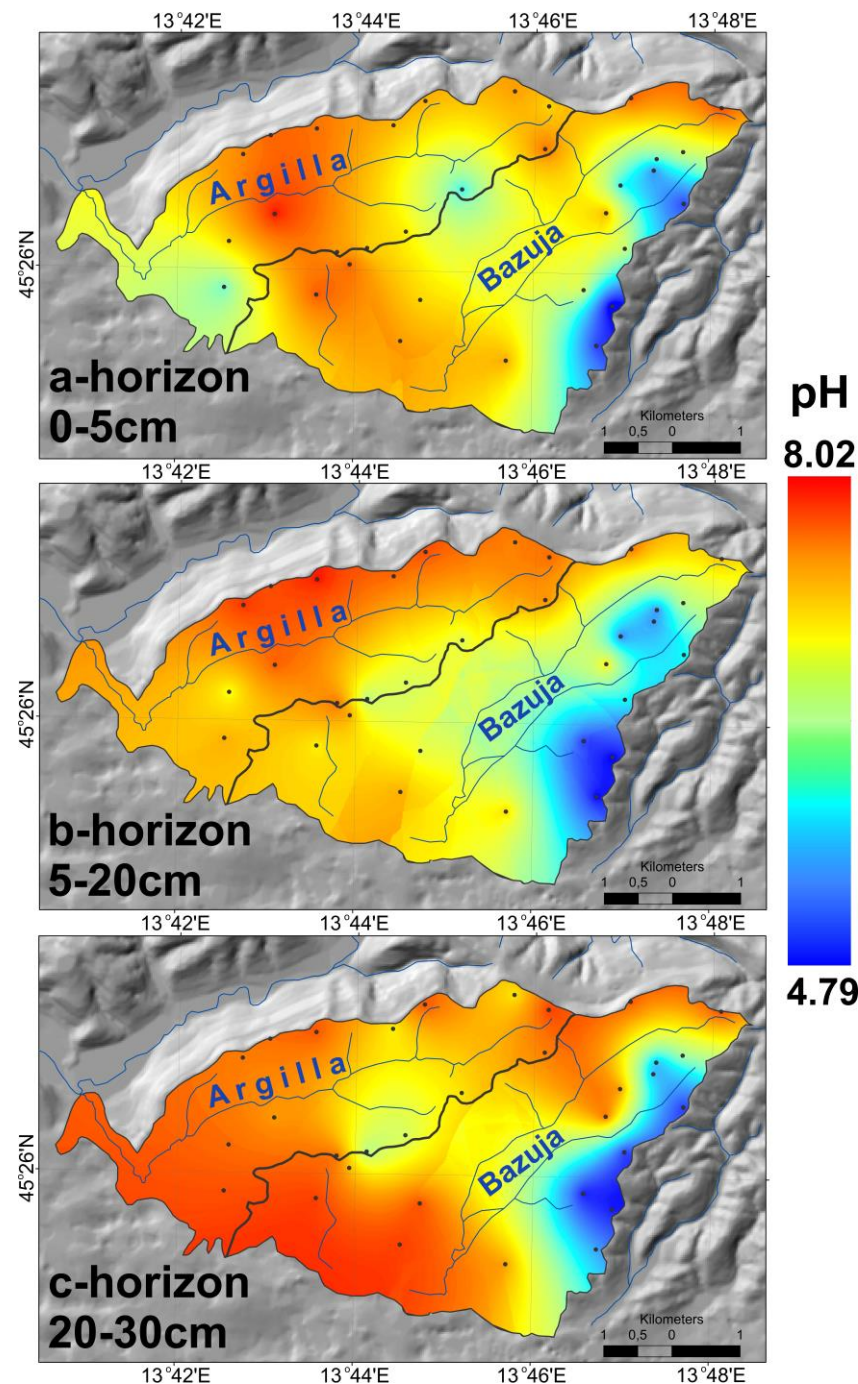


Figure 9. Soil pH_(H₂O) in a, b, and c horizons in both catchments.

It is visible in Table 5 that EIC values are positive (enrichment) in agricultural areas, while forested areas show a loss in EIC values. Therefore, reforestation will reduce erosion rates and the formation of badlands [23], and enhance chemical weathering in the Argilla River catchment. According to [78], significant changes can occur within a period of approximately 100 years. The authors [79] documented, however, that even after only a few decades, there can be changes to the vegetation community and effects on soil organic matter in the planar zone that cause increased chemical weathering [53,79]. The mean EIC values show losses compared with the c-horizon in all base cations in the Bazuja River catchment, while they are enriched in the Argilla River catchment, or they are depleted, but not as much as in the Bazuja River. It can be concluded that chemical weathering is higher in forested areas, while in areas with intensive agricultural activities, chemical weathering

is much lower, or there may even be enrichment. The elemental uptake by biomass is stressed in [21], where the authors point out that weathering rates are considerably affected by botanical uptake. Plant roots and their symbionts can speed up the weathering of rocks by chemically attacking them with a variety of organic acid compounds [80]. This can lower the pH of soil water around roots by up to two units [75]. In addition, organic acids can also form complexes with metals, which can help transfer them from minerals to plants [80]. The effect of plant uptake varies depending on the mineral. For example, the effect is slight for plagioclase but is much greater for mica [21]. Cluster roots can release bursts of exuded carboxylates in soils to free phosphorus or iron from goethite, a mineral that is very slow to weather in the soil environment [81]. Weathering rates in feldspars calculated with included botanical uptake in forested ecosystems are up to five times faster than rates calculated without accounting for the effects of plants [82]. The enrichment of major elements is due to the physical processes that result from losses of topsoil in agricultural soils, which have similar compositions to the parent bedrock in the most weathered parts of the soil.

Table 5. Differences in weathering indices in cultivated areas and forested areas.

EIC Index	a Horizons			b Horizons		
	Cultivated	Old Forest	Young Forest	Cultivated	Old Forest	Young Forest
SiO ₂	7.95	−4.98	−7.93	2.69	−6.10	−3.03
Al ₂ O ₃	7.50	−15.20	−16.25	0.21	−14.48	−7.66
CaO	44.18	−12.40	−36.90	62.64	−20.11	−32.58
MgO	14.39	−20.96	−21.56	2.70	−22.19	−13.56
K ₂ O	21.50	−14.53	−15.24	3.47	−17.92	−9.78
Na ₂ O	12.97	−2.64	−17.15	6.98	−6.84	−11.41
Fe ₂ O ₃	6.36	−14.69	−10.58	0.35	−13.91	−1.61

A comparison of overbank sediments in the river Bazuja swallow hole and stream sediments from the rivers Argilla and Bazuja shows that younger overbank sediments are similar in their composition to the river Bazuja stream sediments. However, overbank sediments sampled in the deeper part of the swallow hole, which were sedimented in the past, show more similarities with recent stream sediments sampled in the river Argilla. This points to the conclusion that older overbank sediments were sedimented in a period when conditions were similar to present-day conditions in the Argilla River catchment, before the Bazuja River catchment was abandoned and sustained intensive agriculture. A small variation in the range of values of the weathering indices of stream sediments, compared with soil sediments, may be due to mineralogical sorting and homogenization during the hydrodynamic and sedimentation processes related to sediment transport. Since the lithologies of the bedrock govern the composition of soils and stream sediments, the small ranges for stream sediment weathering indices may be related to source apportionment. Alternatively, the soils themselves are the primary source for the composition of stream sediment, driven by erosion processes.

6. Conclusions

This research is focused on the chemical weathering of minerals as a result of the changes in land-use and vegetation in the Dragonja River catchment area. Two neighboring catchments were studied: the river Argilla, which is the tributary of the river Dragonja, and the river Bazuja, which is an influent river with allogenic recharge and a wide floodplain in the swallow hole (ponor) zone. Agricultural land-use practice is very intense in the Argilla catchment, while the Bazuja catchment's arable land is mostly abandoned, with progressive forestation. The main objective was to determine the changes in the environment (soil, sediments, and water) in the Dragonja watershed due to natural forestation. Increased forestation causes changes in the hydrological regime, which, in turn, causes changes in soil weathering. Present-day chemical weathering was evaluated with the aid of weathering indices, mass balance (eluvial-illuvial coefficient (EIC) and mass transfer function (MTF)), and strain. By comparing the data calculated by EIC and MTF, it is safe to conclude that

there is no difference in the calculated values. Therefore, it is recommended to use EIC since this method is simpler and faster to use. The abandonment of arable land and intense forestation in the Bazuja catchment caused increased chemical weathering with the loss of base cations (Ca and Mg) and the enrichment of conservative elements (Zr and Ti) in surface horizons. Zn concentrations are lower in the Bazuja catchment, probably due to the increased acidity of water and soil. Increased acidity is caused by base cation loss, induced mainly by plant growth and the production of humic acids. Lead concentration is increased in the Bazuja catchment. It is caused by atmospheric or anthropogenic impact, which has a larger effect on forested areas. Soils in the Argilla River catchment show increased copper concentrations due to vineyard cultivation. Changes in the weathering degree since the formation of the Bazuja River swallow hole until the present show that the oldest overbank sediments are similar to the present-day Argilla River catchment soils. The younger overbank sediments correspond geochemically to the soils of the Bazuja River catchment. This means that chemical and mechanical weathering in the Bazuja catchment is like present-day weathering in the Argilla River catchment, while agriculture is active in the Bazuja River catchment.

Supplementary Materials: The following supporting information can be downloaded at: <https://www.mdpi.com/article/10.3390/land12040913/s1>, Table S1: Major element composition and color of samples.

Author Contributions: Conceptualization, S.M. (Slobodan Miko), Z.P. and O.H.; methodology, S.M. (Slobodan Miko); software, O.H.; validation, Z.P., S.M. (Slobodan Miko) and O.H.; formal analysis, O.H.; investigation, S.M. (Slobodan Miko), Z.P. and O.H.; resources, S.M. (Saša Mesić); data curation, O.H.; writing—original draft preparation, S.M. (Slobodan Miko) and O.H.; writing—review and editing, S.M. (Slobodan Miko), Z.P. and O.H.; visualization, O.H.; project administration, S.M. (Slobodan Miko); funding acquisition, S.M. (Saša Mesić). All authors have read and agreed to the published version of the manuscript.

Funding: This research was funded by the Ministry of Science and Education of Croatia, grant number MZOS-181-1811096-1181.

Data Availability Statement: The data presented in this study are available upon request from the corresponding author.

Acknowledgments: The authors wish to thank all four anonymous reviewers for constructive suggestions and comments that improved our paper.

Conflicts of Interest: The authors declare no conflict of interest. The funders had no role in the design of the study; in the collection, analyses, or interpretation of data; in the writing of the manuscript; or in the decision to publish the results.

References

1. Keesstra, S.D.; van Huissteden, J.; Vandenberghe, J.; Van Dam, O.; de Gier, J.; Pleizier, I.D. Evolution of the Morphology of the River Dragonja (SW Slovenia) Due to Land-Use Changes. *Geomorphology* **2005**, *69*, 191–207. [[CrossRef](#)]
2. Keesstra, S.D.; van Dam, O.; Verstraeten, G.; van Huissteden, J. Changing Sediment Dynamics Due to Natural Reforestation in the Dragonja Catchment, SW Slovenia. *Catena* **2009**, *78*, 60–71. [[CrossRef](#)]
3. Prus, T.; Zupančič, N.; Grčman, H. Soil of the Lower Valley of the Dragonja River (Slovenia). *Acta Agric. Slov.* **2015**, *105*, 61–72. [[CrossRef](#)]
4. Poesen, J.W.A.; Hooke, J.M. Erosion, Flooding and Channel Management in Mediterranean Environments of Southern Europe. *Prog. Phys. Geogr.* **1997**, *21*, 157–199. [[CrossRef](#)]
5. Kelley, D.W.; Nater, E.A. Source Apportionment of Lake Bed Sediments to Watersheds in an Upper Mississippi Basin Using a Chemical Mass Balance Method. *Catena* **2000**, *41*, 277–292. [[CrossRef](#)]
6. Blaikie, P.M.; Brookfield, H.C. (Eds.) *Land Degradation and Society*; Methuen, Milton Park: Abingdon, UK, 1987.
7. Ellis, E.C.; Kaplan, J.O.; Fuller, D.Q.; Vavrus, S.; Goldewijk, K.K.; Verburg, P.H. Used Planet: A Global History. *Proc. Natl. Acad. Sci. USA* **2013**, *110*, 7978–7985. [[CrossRef](#)]
8. Pritchett William, L. *Properties and Management of Forest Soils*; Wiley and Sons Inc.: Hoboken, NJ, USA, 1979.
9. Lawrence, D.; Coe, M.; Walker, W.; Verchot, L.; Vandecar, K. The Unseen Effects of Deforestation: Biophysical Effects on Climate. *Front. For. Glob. Chang.* **2022**, *5*, 756115. [[CrossRef](#)]

10. Nasir Ahmad, N.S.B.; Mustafa, F.B.; Muhammad Yusoff, S.Y.; Didams, G. A Systematic Review of Soil Erosion Control Practices on the Agricultural Land in Asia. *Int. Soil Water Conserv. Res.* **2020**, *8*, 103–115. [CrossRef]
11. Poesen, J. Soil Erosion in the Anthropocene: Research Needs. *Earth Surf. Process. Landf.* **2018**, *43*, 64–84. [CrossRef]
12. Mahmood, A.; Han, J.C.; Ijaz, M.W.; Siyal, A.A.; Ahmad, M.; Yousaf, M. Impact of Sediment Deposition on Flood Carrying Capacity of an Alluvial Channel: A Case Study of the Lower Indus Basin. *Water* **2022**, *14*, 3321. [CrossRef]
13. EFA Eurostat's Annual Data Collection European Forest Accounts (EFA). Available online: https://ec.europa.eu/eurostat/statistics-explained/index.php?title=Forests,_forestry_and_logging#Forests_in_the_EU (accessed on 16 April 2023).
14. Hu, X.; Naess, J.S.; Jordan, C.M.; Huang, B.; Zhao, W.; Cherubini, F. Recent Global Land Cover Dynamics and Implications for Soil Erosion and Carbon Losses from Deforestation. *Anthropocene* **2021**, *34*, 100291. [CrossRef]
15. Bouma, J.; Varallyay, G.; Batjes, N.H. Principal Land Use Changes Anticipated in Europe. *Agric. Ecosyst. Environ.* **1998**, *67*, 103–119. [CrossRef]
16. Kaplan, J.O.; Krumhardt, K.M.; Zimmermann, N. The Prehistoric and Preindustrial Deforestation of Europe. *Quat. Sci. Rev.* **2009**, *28*, 3016–3034. [CrossRef]
17. Dotterweich, M. The History of Human-Induced Soil Erosion: Geomorphic Legacies, Early Descriptions and Research, and the Development of Soil Conservation-A Global Synopsis. *Geomorphology* **2013**, *201*, 1–34. [CrossRef]
18. Borrelli, P.; Robinson, D.A.; Fleischer, L.R.; Lugato, E.; Ballabio, C.; Alewell, C.; Meusburger, K.; Modugno, S.; Schütt, B.; Ferro, V.; et al. An Assessment of the Global Impact of 21st Century Land Use Change on Soil Erosion. *Nat. Commun.* **2017**, *8*, 2013. [CrossRef] [PubMed]
19. Qian, K.; Ma, X.; Wang, Y.; Yuan, X.; Yan, W.; Liu, Y.; Yang, X.; Li, J. Effects of Vegetation Change on Soil Erosion by Water in Major Basins, Central Asia. *Remote Sens.* **2022**, *14*, 5507. [CrossRef]
20. Heckman, K.; Rasmussen, C. Lithologic Controls on Regolith Weathering and Mass Flux in Forested Ecosystems of the Southwestern USA. *Geoderma* **2011**, *164*, 99–111. [CrossRef]
21. Taylor, A.B.; Velbel, M.A. Geochemical Mass Balances and Weathering Rates in Forested Watersheds of the Southern Blue Ridge II. Effects of Botanical Uptake Terms. *Geoderma* **1991**, *51*, 29–50. [CrossRef]
22. Gulam, V.; Pollak, D.; Podolszki, L. The Analysis of the Flysch Badlands Inventory in Central Istria, Croatia. *Geol. Croat.* **2014**, *67*, 1–14. [CrossRef]
23. Gulam, V.; Gajski, D.; Podolszki, L. Photogrammetric Measurement Methods of the Gully Rock Wall Retreat in Istrian Badlands. *Catena* **2018**, *160*, 298–309. [CrossRef]
24. Jovančević, S.D.; Rubinić, J.; Ružić, I.; Radišić, M. Influence of Carbonate-Flysch Contact and Groundwater Dynamics on the Occurrence of Geohazards in Istria, Croatia. *Land* **2021**, *10*, 441. [CrossRef]
25. Bostjančić, I.; Gulam, V.; Frangen, T.; Hečej, N. Relation between Relief and Badland Spatial Distribution in the Paleogene Pazin Basin, Croatia. *J. Maps* **2023**, 1–10. [CrossRef]
26. Keesstra, S.D.; Bruijnzeel, L.A.; van Huissteden, J. Meso-Scale Catchment Sediment Budgets: Combining Field Surveys and Modeling in the Dragonja Catchment, Southwest Slovenia. *Earth Surf. Process. Landf.* **2009**, *34*, 1547–1561. [CrossRef]
27. Halamić, J.; Miko, S.; Peh, Z.; Galović, L.; Šorša, A. *Geochemical Atlas of the Republic of Croatia*; Halamić, J., Miko, S., Eds.; Croatian Geological Survey: Zagreb, Croatia, 2009; ISBN 978-953-6907-18-2.
28. Peh, Z.; Miko, S.; Hasan, O. Geochemical Background in Soils: A Linear Process Domain? An Example from Istria (Croatia). *Environ. Earth Sci.* **2010**, *59*, 1367–1383. [CrossRef]
29. Halamić, J.; Peh, Z.; Miko, S.; Galović, L.; Šorša, A. Geochemical Atlas of Croatia: Environmental Implications and Geodynamical Thread. *J. Geochem. Exp.* **2012**, *115*, 36–46. [CrossRef]
30. Hasan, O.; Miko, S.; Ilijanić, N.; Brunović, D.; Dedić, Ž.; Šparica Miko, M.; Peh, Z. Discrimination of Topsoil Environments in a Karst Landscape: An Outcome of a Geochemical Mapping Campaign. *Geochem. Trans.* **2020**, *21*, 1–22. [CrossRef]
31. Durn, G.; Ottner, F.; Slovenec, D. Mineralogical and Geochemical Indicators of the Polygenetic Nature of Terra Rossa in Istria, Croatia. *Geoderma* **1999**, *91*, 125–150. [CrossRef]
32. Razum, I.; Rubinić, V.; Miko, S.; Ružičić, S.; Durn, G. Coherent Provenance Analysis of Terra Rossa from the Northern Adriatic Based on Heavy Mineral Assemblages Reveals the Emerged Adriatic Shelf as the Main Recurring Source of Siliciclastic Material for Their Formation. *CATENA* **2023**, *226*, 107083. [CrossRef]
33. Durn, G. Terra Rossa in the Mediterranean Region: Parent Materials, Composition and Origin. *Geol. Croat.* **2003**, *56*, 83–100. [CrossRef]
34. Miko, S.; Durn, G.; Prohić, E. Evaluation of Terra Rossa Geochemical Baselines from Croatian Karst Regions. *J. Geochem. Exp.* **1999**, *66*, 173–182. [CrossRef]
35. Peh, Z.; Miko, S.; Bukovec, D. The Geochemical Background in Istrian Soils. *Nat. Croat.* **2003**, *12*, 195–232.
36. Egli, M.; Mirabella, A.; Sartori, G.; Fitze, P. Weathering Rates as a Function of Climate: Results from a Climosequence of the Val Genova (Trentino, Italian Alps). *Geoderma* **2003**, *111*, 99–121. [CrossRef]
37. Anderson, S.P.; Dietrich, W.E.; Brimhall, G.H. Weathering Profiles, Mass-Balance Analysis, and Rates of Solute Loss: Linkages between Weathering and Erosion in a Small, Steep Catchment. *GSA Bull.* **2002**, *114*, 1143–1158. [CrossRef]
38. Munroe, J.S.; Farrugia, G.; Ryan, P.C. Parent Material and Chemical Weathering in Alpine Soils on Mt. Mansfield, Vermont, USA. *Catena* **2007**, *70*, 39–48. [CrossRef]

39. Jin, L.; Ravella, R.; Ketchum, B.; Bierman, P.R.; Heaney, P.; White, T.; Brantley, S.L. Mineral Weathering and Elemental Transport during Hillslope Evolution at the Susquehanna/Shale Hills Critical Zone Observatory. *Geochim. Cosmochim. Acta* **2010**, *74*, 3669–3691. [[CrossRef](#)]
40. Dengiz, O.; Sağlam, M.; Özyaytekin, H.H.; Başkan, O. Weathering Rates and Some Physico-Chemical Characteristics of Soils Developed on a Calcic Toposequences. *Carpathian J. Earth Environ. Sci.* **2013**, *8*, 13–24.
41. Tunçay, T.; Dengiz, O.; Bayramin, I.; Kilic, S.; Başkan, O. Chemical Weathering Indices Applied to Soils Developed on Old Lake Sediments in a Semi-Arid Region of Turkey. *Eurasian J. Soil Sci.* **2019**, *8*, 60–72. [[CrossRef](#)]
42. Nesbitt, H.W.; Young, G.M. Early Proterozoic Climates and Plate Motions Inferred from Major Element Chemistry of Lutites. *Nature* **1982**, *22*, 715–717. [[CrossRef](#)]
43. Fedo, C.M.; Nesbitt, H.W.; Young, G.M. Unravelling the Effects of Potassium Metasomatism in Sedimentary Rocks and Paleosols, with Implications for Paleoweathering Conditions and Provenance. *Geology* **1995**, *23*, 921–924. [[CrossRef](#)]
44. Harnois, L. The CIW Index: A New Chemical Index of Weathering. *Sediment. Geol.* **1988**, *55*, 319–322. [[CrossRef](#)]
45. Parker, A. An Index of Weathering for Silicate Rocks. *Geol. Mag.* **1970**, *107*, 501–504. [[CrossRef](#)]
46. Muir, J.W.; Logan, J. Eluvial/Illuvial Coefficients of Major Elements and the Corresponding Losses and Gains in Three Soil Profiles. *J. Soil Sci.* **1982**, *33*, 295–308. [[CrossRef](#)]
47. Birkeland, P.W. *Soils and Geomorphology*; Oxford University Press: New York, NY, USA, 1999.
48. Merritts, D.J.; Chadwick, O.A.; Hendricks, D.M.; Brimhall, G.H.; Lewis, C.J. The Mass Balance of Soil Evolution on Late Quaternary Marine Terraces, Northern California. *Geol. Soc. Am. Bull.* **1992**, *104*, 1456–1470. [[CrossRef](#)]
49. Price, J.R.; Velbel, M.A. Chemical Weathering Indices Applied to Weathering Profiles Developed on Heterogeneous Felsic Metamorphic Parent Rocks. *Chem. Geol.* **2003**, *202*, 397–416. [[CrossRef](#)]
50. Land, M.; Öhlander, B. Chemical Weathering Rates, Erosion Rates and Mobility of Major and Trace Elements in a Boreal Granitic Till. *Aquat. Geochem.* **2000**, *6*, 435–460. [[CrossRef](#)]
51. Jacobs, P.M.; Davis, A.T. Mineralogical and Geochemical Evidence of Weathering in a Middle to Late Pleistocene Paleosol Sequence in the Driftless Area of Wisconsin. *Quat. Res.* **2018**, *89*, 756–768. [[CrossRef](#)]
52. Heidari, A.; Raheb, A. Geochemical Indices of Soil Development on Basalt Rocks in Arid to Sub-Humid Climosequence of Central Iran. *J. Mt. Sci.* **2020**, *17*, 1652–1669. [[CrossRef](#)]
53. Musso, A.; Tikhomirov, D.; Plötze, M.L.; Greinwald, K.; Hartmann, A.; Geitner, C.; Maier, F.; Petibon, F.; Egli, M. Soil Formation and Mass Redistribution during the Holocene Using Meteoric ^{10}Be , Soil Chemistry and Mineralogy. *Geosciences* **2022**, *12*, 99. [[CrossRef](#)]
54. Owens, P.N.; Walling, D.E.; Leeks, G.J.L. Use of Floodplain Sediment Cores to Investigate Recent Historical Changes in Overbank Sedimentation Rates and Sediment Sources in the Catchment of the River Ouse, Yorkshire, UK. *Catena* **1999**, *36*, 21–47. [[CrossRef](#)]
55. Egli, M.; Fitze, P. Formulation of pedologic mass balance based on immobile elements: A revision. *Soil Sci.* **2000**, *165*, 437–443. [[CrossRef](#)]
56. Bergant, S.; Tišljarić, J.; Šparica, M. Eocene Carbonates and Flysch Deposits of the Pazin Basin. In *Field Trip Guidebook: Evolution of Depositional Environments from the Palaeozoic to the Quaternary in the Karst Dinarides and the Pannonian Basin/22nd IAS Meeting of Sedimentology*; Vlahović, I., Tišljarić, J., Eds.; Institut za Geološka Istraživanja: Zagreb, Croatia, 2003; pp. 57–64.
57. Marinčić, S.; Šparica, M.; Tunis, G.; Uchman, A. The Eocene Flysch Deposits of the Istrian Peninsula in Croatia and Slovenia: Regional, Stratigraphic, Sedimentological and Ichtiological Analyses. *Annales* **1996**, *9*, 435–460.
58. Magdalenčić, Z. Sedimentologija Flišnih Naslaga Srednje Istre (Sedimentology of Central Istria Flysch Deposits). *Acta Geol.* **1972**, *VII*, 34.
59. Makjanić, B.; Volarić, B. Kratki Pregled Klime Istre. In *Liburnijske Teme*; Katedra Čakavskog Sabora: Opatija, Croatia, 1981; pp. 93–101.
60. Stolbovov, V.; Montanarella, L.; Filippi, N.; Jones, A.; Gallego, J.; Grassi, G. *Soil Sampling Protocol to Certify the Changes of Organic Carbon Stock in Mineral Soils of European Union, Version 2*; Office for Official Publications of the European Communities: Luxembourg, 2007; Volume 21576, ISBN 9783540892076.
61. Swennen, R.; Van Der Sluys, J.; Hindel, R.; Brusselmans, A. Geochemistry of Overbank and High-Order Stream Sediments in Belgium and Luxembourg: A Way to Assess Environmental Pollution. *J. Geochem. Exp.* **1998**, *62*, 67–79. [[CrossRef](#)]
62. Blake, G.R. Bulk Density. In *Methods of Soil Analysis, Part 4*; American Society of Agronomy: St. Paul, MN, USA, 2003; p. 1692.
63. White, A.F.; Blum, A.E. Effects of Climate on Chemical Weathering in Watersheds. *Geochim. Cosmochim. Acta* **1995**, *59*, 1729–1747. [[CrossRef](#)]
64. Melkerud, P.A.; Bain, D.C.; Olsson, M.T. Historical Weathering Based on Chemical Analyses of Two Spodosols in Southern Sweden. *Water Air Soil Pollut. Focus* **2003**, *3*, 49–61. [[CrossRef](#)]
65. Stiles, C.A.; Mora, C.I.; Driese, S.G. Pedogenic Processes and Domain Boundaries in a Vertisol Climosequence: Evidence from Titanium and Zirconium Distribution and Morphology. *Geoderma* **2003**, *116*, 279–299. [[CrossRef](#)]
66. Brimhall, G.H.; Dietrich, W.E. Constitutive Mass Balance Relations between Chemical Composition, Volume, Density, Porosity, and Strain in Metasomatic Hydrochemical Systems: Results on Weathering and Pedogenesis. *Geochim. Cosmochim. Acta* **1987**, *51*, 567–587. [[CrossRef](#)]
67. Brimhall, G.H.; Chadwick, O.A.; Lewis, C.J.; Compston, W.; Williams, I.S.; Danti, K.J.; Dietrich, W.E.; Power, M.E.; Hendricks, D.; Bratt, J. Deformational Mass Transport and Invasive Processes in Soil Evolution. *Science* **1992**, *255*, 695–702. [[CrossRef](#)]

68. Retallack, G. *Soils of the Past, an Introduction to Paleopedology*; Uniwiv Hyman: Boston, MA, USA, 1990; ISBN 9789896540821.
69. Nesbitt, H.W.; Markovics, G.; Price, R. Chemical Processes Affecting Alkalis and Alkaline Earths during Continental Weathering. *Geochim. Cosmochim. Acta* **1980**, *44*, 1659–1666. [[CrossRef](#)]
70. Dixon, J.L.; von Blanckenburg, F. Soils as Pacemakers and Limiters of Global Silicate Weathering. *Comptes Rendus Geosci.* **2012**, *344*, 597–609. [[CrossRef](#)]
71. Ferrier, K.L.; Kirchner, J.W. Effects of Physical Erosion on Chemical Denudation Rates: A Numerical Modeling Study of Soil-Mantled Hillslopes. *Earth Planet. Sci. Lett.* **2008**, *272*, 591–599. [[CrossRef](#)]
72. Ma, L.; Jin, L.; Brantley, S.L. How Mineralogy and Slope Aspect Affect REE Release and Fractionation during Shale Weathering in the Susquehanna/Shale Hills Critical Zone Observatory. *Chem. Geol.* **2011**, *290*, 31–49. [[CrossRef](#)]
73. Velbel, M.A.; Price, J.R. Solute Geochemical Mass-Balances and Mineral Weathering Rates in Small Watersheds: Methodology, Recent Advances, and Future Directions. *Appl. Geochem.* **2007**, *22*, 1682–1700. [[CrossRef](#)]
74. Ampong, K.; Thilakaranthna, M.S.; Gorim, L.Y. Understanding the Role of Humic Acids on Crop Performance and Soil Health. *Front. Agron.* **2022**, *4*, 1–14. [[CrossRef](#)]
75. Lucas, Y. The Role of Plants in Controlling Rates and Products of Weathering: Importance of Biological Pumping. *Annu. Rev. Earth Planet. Sci.* **2001**, *29*, 135–163. [[CrossRef](#)]
76. Egli, M.; Dahms, D.; Norton, K. Soil Formation Rates on Silicate Parent Material in Alpine Environments: Different Approaches—Different Results? *Geoderma* **2014**, *213*, 320–333. [[CrossRef](#)]
77. Miko, S.; Miko Šparica, M.; Hasan, O.; Peh, Z.; Mesić, S.; Bukovec, D. Lead Pollution of the Croatian Mountain Karst Soils Caused by Acid Rain Deposition; Evidence from Geochemical Mapping and Lead Isotopes. In *Acid Rain 2005; Conference Abstracts*; Huntova, I., Ostatnicka, J., Dostalova, Z., Navratil, T., Eds.; Czech Hydrometeorological Institute: Prague, Czech Republic, 2005; p. 111.
78. Haeberli, W.; Hoelzle, M.; Paul, F.; Zemp, M. Integrated Monitoring of Mountain Glaciers as Key Indicators of Global Climate Change: The European Alps. *Ann. Glaciol.* **2007**, *46*, 150–160. [[CrossRef](#)]
79. Zanelli, R.; Egli, M.; Mirabella, A.; Giaccai, D.; Abdelmoula, M. Vegetation Effects on Pedogenetic Forms of Fe, Al and Si and on Clay Minerals in Soils in Southern Switzerland and Northern Italy. *Geoderma* **2007**, *141*, 119–129. [[CrossRef](#)]
80. Porder, S. How Plants Enhance Weathering and How Weathering Is Important to Plants. *Elements* **2019**, *15*, 241–246. [[CrossRef](#)]
81. Lambers, H.; Nascimento, D.L.; Oliveira, R.S.; Shi, J. Do Cluster Roots of Red Alder Play a Role in Nutrient Acquisition from Bedrock? *Proc. Natl. Acad. Sci. USA* **2019**, *116*, 11575–11576. [[CrossRef](#)] [[PubMed](#)]
82. Velbel, M.A. Geochemical Mass Balances and Weathering Rates in Forested Watersheds of the Southern Blue Ridge. *Am. J. Sci.* **1985**, *285*, 904–930. [[CrossRef](#)]

Disclaimer/Publisher’s Note: The statements, opinions and data contained in all publications are solely those of the individual author(s) and contributor(s) and not of MDPI and/or the editor(s). MDPI and/or the editor(s) disclaim responsibility for any injury to people or property resulting from any ideas, methods, instructions or products referred to in the content.